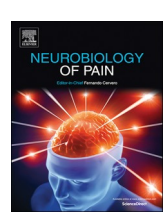
ELSEVIER

Contents lists available at ScienceDirect

Neurobiology of Pain

journal homepage: www.elsevier.com/locate/ynpai



The naked mole-rat has a functional purinergic pain pathway despite having a non-functional peptidergic pain pathway



Brigitte M. Browe^a, Abigail R. Olsen^a, Cesar Ramirez^a, Rebecca H. Rickman^b, Ewan St. John Smith^b, Thomas J. Park^a,*

ARTICLE INFO

Keywords:
P2X3 receptor
Nociception
Naked mole-rat
Cannabinoid
purinergic C-fibers

ABSTRACT

Naked mole-rats (Heterocephalus glaber) have adaptations within their pain pathway that are beneficial to survival in large colonies within poorly ventilated burrow systems, with lower O2 and higher CO2 ambient levels than ground-level environments. These adaptations ultimately lead to a partial disruption of the C-fiber pain pathway, which enables naked mole-rats to not feel pain from the acidosis associated with CO₂ accumulation. One hallmark of this disruption is that naked mole-rats do not express neuropeptides, such as Substance P and calcitonin gene-related peptide in their cutaneous C-fibers, effectively making the peptidergic pain pathway hypofunctional. One C-fiber pathway that remains unstudied in the naked mole-rat is the non-peptidergic, purinergic pathway, despite this being a key pathway for inflammatory pain. The current study aimed to establish the functionality of the purinergic pathway in naked mole-rats and the effectiveness of cannabinoids in attenuating pain through this pathway. Cannabinoids can manage chronic inflammatory pain in both humans and mouse models, and studies suggest a major downstream role for the purinergic receptor, P2X3, in this treatment. Here we used Ca²⁺-imaging of cultured dorsal root ganglion neurons and in vivo behavioral testing to demonstrate that the P2X3 pathway is functional in naked mole-rats. Additionally, formalin-induced inflammatory pain was reduced by the cannabinoid receptor agonist, WIN55 (inflammatory, but not acute phase) and the P2X3 receptor antagonist A-317491 (acute and inflammatory phases). This study establishes that the purinergic C-fiber pathway is present and functional in naked mole-rats and that cannabinoid-mediated analgesia occurs in this species.

1. Introduction

The African naked mole-rat (*Heterocephalus glaber*) is a eusocial, subterranean rodent with adaptations that make this species resistant to a multitude of noxious stimuli (LaVinka and Park, 2012; Smith et al., 2020). This includes immunity to the burning pain associated with capsaicin, the spicy compound in chili peppers (Park et al., 2008; Eigenbrod et al., 2019). Normally, capsaicin activates the transient receptor potential vanilloid 1 (TRPV1) ion channel, which is predominantly expressed by unmyelinated C-fiber sensory neurons that also express neuropeptides (i.e. peptidergic C-fibers). Due to their pseudounipolar morphology, activation of TRPV1⁺ neurons results in release of neuropeptides (e.g. Substance P and calcitonin gene-related peptide, SP and CGRP) both at the periphery and in the spinal cord (Cavanaugh et al., 2011; Rigoni et al., 2009; Eberhardt et al., 2017). In

most mammals, TRPV1 + peptidergic C-fibers synapse in lamina I of the spinal cord where the neurokinin I receptor (NK1r) for SP is also expressed and the SP – NK1r pathway is important for transmission of the pain signal from the periphery to the central nervous system (Todd, 2010). While TRPV1 is expressed at similar levels in naked mole-rat and mouse sensory neurons, and has similar activation properties, naked mole-rat TRPV1 + fibers synapse with a greater frequency to neurons in deeper spinal cord laminae than in the mouse (Park et al., 2008; Smith et al., 2011; Omerbasic et al., 2016). Experiments involving immunohistochemistry and intrathecal administration of SP showed that the behavioral insensitivity to capsaicin is attributable to a lack of neuropeptides in C-fibers of the naked mole-rat, effectively making the TRPV1 pain pathway non-functional with regard to pain signaling (Brand et al., 2010; Park et al., 2003, 2008).

Consistent with a lack of pain-associated neuropeptides in TRPV1 +

E-mail address: tpark@uic.edu (T.J. Park).

^a Laboratory of Integrative Neuroscience, Department of Biological Sciences, University of Illinois at Chicago, Chicago, IL, USA

^b Department of Pharmacology, University of Cambridge, Cambridge CB2 1PD, UK

^{*}Corresponding author at: University of Illinois at Chicago, Laboratory of Integrative Neuroscience, Department of Biological Sciences, 840 West Taylor St, Chicago, Illinois 60607, USA.

C-fibers, naked mole-rats show a reduced response to formalin-induced nocifensive behaviors (Park et al, 2008). In particular, naked mole-rats have a longer, yet significantly less intense, response to cutaneous injection of the irritant formalin, particularly during the second pain phase (Phase II; Park et al., 2008; Ma et al., 2015). Phase II is considered an inflammatory pain that, in mice and humans, is predominantly mediated by central sensitization of spinal dorsal horn neurons as a result of the barrage of C-fiber input during the early phase (Phase I) (Coderre et al., 1993; Dickenson and Sullivan, 1987; Raboisson et al., 1995; Shibata et al., 1989; Park et al., 2008; Dulu et al., 2014; Hunskaar and Hole, 1987). Importantly, although naked mole-rats show a reduced response to formalin, it is not completely absent, indicating that there is still a portion of the inflammatory pain pathway that is intact. However, it is currently unknown which receptors mediate this pain response in naked mole-rats.

Here we consider the other major C-fiber population, non-peptidergic neurons that, compared to peptidergic C-fibers, express high levels of the purinergic ATP receptor P2X3 and bind isolectin B4 (IB4) (Cauwels et al., 2014; Oliveira et al., 2009; Zeisel et al., 2018; Viatchenko-Karpinski et al., 2016). Previously, we have shown that a similar proportion of mouse and naked mole-rat dorsal root ganglion (DRG) neurons bind IB4 and that these neurons synapse in laminae II of the dorsal horn (Park et al., 2008) where non-peptidergic C fibers normally synapse (Todd, 2010). Considering the lamina I vs. lamina II input of peptidergic vs. non-peptidergic C-fibers, it is thus possible that the non-peptidergic, P2X3r⁺ C-fibers mediate the (albeit diminished) formalin-induced pain response in naked mole-rats. Therefore, the first objective in this study was to examine the functionality of the P2X3r pathway in naked mole-rats and determine its role in formalin-induced pain.

The possibility that naked mole-rats rely on the P2X3r pathway to mediate inflammatory pain could be a valuable tool in analyzing how analgesic treatments influence pain in the absence of a functional peptidergic pathway. Because analgesic treatments with cannabinoids have been used to effectively reduce inflammatory pain (Calignano et al., 1998), we also decided to test the naked mole-rats with a cannabinoid receptor agonist and antagonist.

Cannabinoids function through the endocannabinoid system, which is a retrograde synaptic signaling pathway with analgesic effects that have been identified in the dorsal horn of the spinal cord (Kreitzer and Regehr, 2002; Chiou et al., 2013). Cannabinoids mediate their analgesic effects through cannabinoid receptor 1 (CB1r), which is predominantly expressed by neurons, whereas CB2r is strongly expressed by cells of the immune system (Tsou et al., 1996; Hohmann et al., 1999; Agarwal et al., 2007; Herkenham et al., 1991; Martin et al., 1995, 1996; Nackley et al., 2003). Inflammation increases CB1r expression in C-fibers, but not A-fibers, thus further supporting the hypothesis that cannabinoidmediated analgesia in inflammatory pain primarily occurs via C-fibers (Amaya et al., 2006; Evans et al., 2004). Attenuation of pain by cannabinoids has been described in the C-fiber pathways of both peptidergic (i.e. TRPV1 +) and purinergic (i.e. P2X3r +) nerves, through CB1r activation on the axon terminals in the dorsal horn of the spinal cord (Nerandzic et al., 2018; Starowicz et al., 2013). Studies in mice where CB1r was knocked out specifically in primary sensory neurons showed a reduced analgesic effect of the CB1/2r agonist WIN 55212-2 in inflammatory pain assays compared to the effect observed in wild type mice, thus suggesting a key role for CB1r expressed by sensory neurons in cannabinoid-mediated analgesia (Agarwal et al., 2007).

However, the mechanisms underpinning cannabinoid analgesia are not well understood. It was initially thought that cannabinoid inhibition of TRPV1 presented a good target for pain therapeutics, but results demonstrated a complicated picture. For example, TRPV1-mediated release of neuropeptides can be inhibited by CB1r activation (an antinociceptive effect), as well as TRPV1 being directly activated by the endocannabinoid N-arachidonoylethanolamine (AEA, a pro-nociceptive effect), thus indicating that cannabinoids produce both pro- and anti-

nociceptive effects via TRPV1 (Carey et al., 2016). Previous research also suggests that activation of CB1r can directly inhibit inflammatory pain through P2X3r, as shown by inhibition of the hyperalgesic response to mechanical stimuli and Ca^{2+} influx in small diameter DRG neurons after α, β -met-ATP (ATP, a P2X3r agonist) administration both *in vivo* and *in vitro* (Oliveira-Fusaro et al., 2017). Due to the complex nature of cannabinoid interactions with TRPV1/peptidergic neurons, using a model system in which the TRPV1/peptidergic system is hypofunctional, such as the naked mole-rat, provides an opportunity to determine the degree to which the P2X3r/non-peptidergic pathway contributes to cannabinoid mediated analgesia. Therefore, the second objective of this study was to examine cannabinoid effects on P2X3r-mediated responses in the naked mole-rat.

We find that naked mole-rats do have a functional purinergic pain pathway that can be stimulated by activating P2X3r. Additionally, cannabinoids are able to attenuate pain caused by stimulation of the P2X3r. However, there does not appear to be an inflammatory pain response after stimulating the P2X3r pathway, indicating some disruption in the inflammatory pathway of naked mole-rats.

2. Methods

2.1. Animals

All mice used for behavioral studies and spinal cord immunohistochemistry at the University of Illinois at Chicago were 2-5month-old C57BL/6J males, which were bred from stock, originally obtained from Charles River Laboratories, Wilmington, Massachusetts, USA. Mice were kept in a temperature-controlled environment of 22 °C with a 12-hour light/dark cycle. Naked mole-rats of both sexes were born in colonies maintained at the University of Illinois at Chicago. Naked mole-rats were kept at a controlled temperature (27 °C) and humidity (50–60%) with a 12-hour light/dark cycle. For Ca²⁺-imaging and DRG neuron immunohistochemistry studies at the University of Cambridge, both male and female adult C57BL/6J (Envigo) mice (8-12 weeks) and naked mole-rats (9-24 months) were used. Mice were kept under 12-hour light/dark cycle in a temperature-controlled (21 °C) room, and naked mole-rats were maintained in a temperature-controlled (28-32 °C) room and kept under red lighting (08:00-16:00). In both Chicago and Cambridge, animals had access to water (in the case of mice) and food ad libitum. Mice were housed in standard mouse cages and naked mole-rat colonies were housed in bespoke caging systems consisting of mouse and rat cages connected by tunnels (Artwohl et al., 2002). All procedures were conducted according to the animal protocols approved by the University of Illinois at Chicago Institutional Animal Care and Use Committee or under a Home Office Project License (P7EBFC1B1), conducted in accordance with the UK Animals (Scientific Procedures) Act 1986 Amendment Regulations 2012 and reviewed by the University of Cambridge Animal Welfare and Ethical Review Body.

2.2. Drug Preparation

Formalin Preparation. 37% stock formaldehyde solution was purchased from Sigma-Aldrich and diluted in water to 2% by volume. WIN 55212-2 CB1r Agonist Preparation. WIN 55212-2 mesylate salt (WIN55) was obtained from Sigma-Aldrich and suspended at 1 mg/mL in 49.5% TEG, 49.5% Saline, 0.5% DMSO, and 0.5% Cremaphor and ready to be diluted to injection concentrations with saline. Dilutions were injected at either 1.5 mg/kg or 3 mg/kg or saline vehicle. SP Preparation. We used dilutions in accordance with Park et al., 2008. Briefly, 100 μM of SP was dissolved in 0.9% Saline. A-317491 P2X3r Antagonist Preparation. A-317491 was diluted in 0.9% Saline and given at a dose of 50 μg/10 μL. α-β-metATP (ATP) P2X3r Agonist Preparation. ATP was diluted to 50 μM/10 μL in 0.9% Saline.

2.3. Drug conditions

An insulin syringe was used to administer all drugs. For cannabinoid experiments, drugs were injected via intraperitoneal (IP) administration 30 min prior to the commencement of behavioral tests and syringes contained either a 1.5 mg/kg, or a 3 mg/kg dose of WIN55, or a 0.9% dose of saline. SP was injected by intrathecal administration between the L4 and L5 vertebrae at 20 μL volume 30 min prior to testing. For the P2X3r antagonist, 40 μM of A-317491 was injected into the dorsal paw 10 min prior to beginning the formalin test. 10 μL of ATP was injected to the plantar side of the hind paw 10 min prior to the first von Frey test.

2.4. Formalin test

Each mouse and naked mole-rat received 15–20 μ L of formalin (2%) subcutaneously into the dorsal side of the hind paw with an insulin syringe. The animal was placed into an empty mouse cage without a lid and observed for 90 min. Licking, biting, and lifting of the formalin injected foot were operationally defined as nociceptive behavior. The time spent performing nociceptive behaviors was recorded for all animals in intervals of 5 min for the entire 90-minute duration. The total time observed was divided into 0–10 min (Phase I) for both naked molerats and mice. However, the late phase was defined as 10–60 min for mice and 10–90 min for naked mole-rats due to species differences in reaction to formalin (Eigenbrod et al., 2019). The formalin test was performed and scored by an observer blinded to experimental conditions

2.5. Tail flick

Mice and naked mole-rats were acclimated to a plastic restraint cone where they were placed in it and given a sugar treat daily for 1 week prior to testing. Animals were given a treatment of either saline (control), 1.5 mg/kg WIN55, or 3 mg/kg WIN55 by IP injection 30 min prior to testing. Each animal was tested at all three experimental conditions with at least 48 h between treatments. To test heat sensitivity, a water bath was prepared with water held at 48 °C. Animals were placed in a restraint cone with the tail remaining free from the restraint and when restrained and calm the experimenter lowered the tail into the water and recorded the time in seconds it took for the animal to attempt to remove the tail from the water.

2.6. Von Frey

Mice and naked mole-rats were injected with saline or WIN55 by IP injection 30 mins prior to injection of α - β -met-ATP in the plantar surface of the left hind paw. Sensitivity to mechanical stimuli was assessed using calibrated von Frey filaments (Stoelting, Wood Dale, IL). Animals were placed in 10 cm diameter wire bottom apparatus. The von Frey filaments (0.4–15.1 g) were applied to the mid-plantar surface of each hind paw. The mechanical stimulus producing the 50% paw withdrawal threshold was determined using the up-down method (Chaplan et al., 1994). Behavioral tests using mechanical stimuli were performed on both the ipsilateral and contralateral paw at 10 and 180 min after intraplantar injection of saline or α - β -met-ATP. Each animal was tested with both IP saline and WIN55, and thus served as their own controls.

2.7. Behavioral analysis

All behavioral data was compiled into Microsoft Excel for initial processing. Statistical analysis was done using vassarstats.com T-test and ANOVA calculators.

2.8. Immunohistochemistry

For spinal cord immunohistochemistry, mice and naked mole-rats were decapitated, and spinal cords were quickly removed and fixed with a fixative containing 4% paraformaldehyde (PFA) in 0.1 M phosphate-buffer (PBS, pH 7.4) overnight, and subsequently cryoprotected in 30% sucrose (in PBS). Brains were sectioned coronally (26 µm thickness) on a cryo-microtome and directly placed on slides. Nonspecific immunoreactivity was suppressed by incubating our specimens in a cocktail of 5% normal donkey serum (Jackson), 1% bovine serum albumin (BSA, Sigma) and 0.3% Triton X-100 in PB for an hour at 22-24 °C. CB1r was stained using a rabbit anti-CB1r antibody (Synaptic signaling 1:1000) and P2X3r was stained using a guinea pig anti-P2X3r antibody (Sigma, 1:50). Neuron nuclei were stained using Hoechst (1:1000). Primary antibodies were counterstained with AlexaFluor 488 anti-rabbit (1:1000), and Cy3 anti-guinea pig (1:1000). Glass-mounted sections were cover slipped with Aquamount (Dako, Glosstrup, Denmark). Images acquired on a Fluoview FV 10i confocal laser-scanning microscope (Olympus). Colocalization was analyzed using the FV 10i internal software to determine Pearson's Coefficient and Overlap of CB1r and P2X3r staining. Significant colocalization was set as any correlation coefficient over 0.5 or 50% and referred to as a relatively strong positive overlap. Correlation coefficients > 0.7 or 70% were considered as having a strong positive overlap. The percentage of dorsal horn images with these two standards of overlap were compiled for each species.

For immunohistochemistry with DRG neurons, mice and naked mole-rats were euthanized by cervical dislocation (mice) or a rising concentration of CO2 and decapitation (naked mole-rats) according to local procedures. Thoracolumbar (TL) DRG were dissected and fixed in Zamboni's fixative (2% paraformaldehyde and 15% picric acid in sodium phosphate buffer; 1 h). DRG were then cryoprotected overnight in 30% sucrose (in PBS) at 4 °C, before embedding in ShandonTM M-1 Embedding Matrix (Thermo Fisher Scientific) and snap frozen in liquid nitrogen before being then stored at -80 °C. Embedded DRG were sectioned (12 µm) using a Leica Cryostat (CM3000; Nussloch, Germany), and mounted on Superfrost Plus microscope slides (Thermo Fisher Scientific). Sections were stored at -20 °C until further use. Slides were defrosted, washed with PBS-tween (PBS-T) and blocked in antibody diluent solution (1% BSA, 5% donkey serum (Sigma-Aldrich), and 0.2% Triton X-100 (Sigma-Aldrich) in PBS; 1 h) at room temperature. All sections were incubated overnight (4 °C, humid atmosphere) with primary antibodies prepared in diluent. Primary antibodies used were rabbit anti-P2X3r polyclonal (1:1000, Alomone) and guinea pig anti-TRPV1 polyclonal (1:500, Alomone). Slides were washed three times using PBS-T before incubation in the appropriate species-specific fluorophore-conjugated secondary antibodies (donkey anti-rabbit IgG-AF350 (Invitrogen); donkey anti-guinea-pig IgG-AF594 (Jackson Lab) for 2 h at room temperature (20-22 °C). All secondary antibodies were used at a 1:1000 dilution. For each antibody, a negative control experiment excluding primary antibody incubation was also performed and showed no staining. Slides were washed in PBS-T, mounted using Mowiol-based mounting media. Sections were imaged with an Olympus BX51 microscope (Tokyo, Japan). Brightfield and fluorescent images were acquired at 10 × and 20 × magnification using a Q-Imaging camera and software (Surrey, Canada). Exposure levels were kept constant for each slide and the same contrast enhancements were made to all slides.

2.9. Primary DRG neuron culture

Mice were killed by cervical dislocation and naked mole-rats were immobilized using a rising concentration of CO₂ and then decapitated according to local procedures. For each animal, a primary DRG neuron culture was prepared using a mixture of TL DRG. The spinal column was dissected and T1-L6 DRG were collected, trimmed of connective fibers,

and placed in ice-cold dissociation media containing L-15 Medium (1X) + GlutaMAX-1 (Life Technologies), supplemented with 24 mM NaHCO3. media (Thermo Fisher Scientific, UK). Harvested DRG were then incubated in 3 mL type 1A collagenase (1 mg/mL with 6 mg/mL bovine serum albumin (BSA in dissociation media; Sigma-Aldrich) for 20 min at 37 °C (mouse) or 32 °C (NMR) in an incubator with 5% CO₂; NMRs are cold-blooded and are maintained at 28 - 32 °C and hence this temperature was used for preparing and maintaining NMR DRG neuron cultures. This was followed by a 30-minute incubation in 3 mL trypsin solution (1 mg/mL with 6 mg/mL BSA in dissociation media; Sigma-Aldrich) at respective temperatures. After removing the enzymes, DRG were placed in 2 mL of DRG culture media composed of L-15 Medium (1X) + GlutaMAX, 10% fetal bovine serum (Sigma-Aldrich), 24 mM NaHCO₃, 38 mM glucose, and 2% penicillin/streptomycin (Life Technologies, UK). DRG neurons were dissociated via gentle mechanical trituration using 1 mL Gilson pipette tips, by pipetting up and down approximately 8 times. Following a 30 s centrifugation at 160 × g (Biofuge primo, Heraeus Instruments; Hanau, Germany) the supernatant containing dissociated cells was collected in a fresh tube, and the remaining pellet was resuspended in 2 mL of media. This process of trituration, centrifugation and collection was repeated a total of five times. Following a 5-minute centrifugation at 160×g, the pellet was resuspended in media and plated onto poly-D-lysine-coated 35 mm glass- bottom dishes (MatTek Corporation, USA) coated with laminin (20 μg/mL; Life Technologies) and were incubated at 37 °C (mouse) and 32 °C (NMR) in 5% CO2 for 20-24 h. The cells were flooded with fresh media after 3 h.

2.10. Ca²⁺-imaging

A day after the preparation of the primary DRG neuron culture, neurons plated on coverslips were loaded with the fluorescent Ca²⁺ indicator Fluo-4 (10 µM; Thermo Fisher Scientific) in extracellular solution (ECS; 140 mM NaCl, 4 mM KCl, 2 mM CaCl2, 1 mM MgCl2, 10 mM HEPES, 4 mM glucose; adjusted to pH 7.4 with NaOH and 300-310 mOsm with sucrose) for 45 min at room temperature. Coverslips were washed once with ECS and placed in an imaging chamber (RC-26, Warner Instruments, UK) and incubated for 5 min with either 0.0102% DMSO (highest concentration used for vehicle/ control for WIN55), 3 µM ACEA (Tocris), 1 nM or 100 nM WIN55. Cells were imaged using a Nikon Eclipse Ti microscope and a $10 \times$ objective. Fluo-4 was excited using a 470 nm LED (Cairn Research, UK) and fluorescent images were acquired every second using a Zyla sCMOS camera (Andor, UK) and Micro-Manager software (v 1.4; National Institute of Health). For all conditions, neurons were initially perfused with whichever prior solution they were incubated in for the final 30 s of the 5 min incubation, then perfused with $\alpha\beta$ -met-ATP (30 μ M, 20 s) and washed with ECS (240 s) before a 20 s KCl (50 mM) stimulus which was applied at the end of every experiment to determine cell viability. Unless otherwise specified, all chemicals and drugs were obtained from Sigma- Aldrich.

2.11. P2X3r and TRPV1 receptor expression in DRG neurons

To determine the expression of P2X3r and TRPV1 in DRG neurons, 2–5 DRG sections were chosen using a random number generator for analysis per each imaged DRG using Fiji/ImageJ (National Institute of Health). Regions of interest (ROI) were drawn around the borders of all neuron cell bodies that were identified morphologically using the brightfield image. The criteria for determining a DRG neuron cell body were they had to have a clear circular outline and a nucleus. Mean fluorescent intensities of the ROIs were measured for the fluorescent channels corresponding to P2X3r and TRPV1. For each section, background fluorescence was subtracted from ROI fluorescent intensities. For each section, $F_{\rm min}$ and $F_{\rm max}$ were determined from ROIs with the lowest ("negative") and highest background-subtracted fluorescent

intensities, respectively. For each experiment, the average F_{min} and F_{max} was determined by taking the mean of all F_{min} and F_{max} . Normalized fluorescence was calculated as (F - average F_{min})/(average F_{max} - average F_{min}). For each animal group, the threshold used for scoring a neuron as positive was set as the normalized minimum grey value across all sections +1 times SD. Each ROI with a normalized fluorescence above the threshold was counted as being immunoreactive and the percentage of P2X3r and TRPV1-positive neurons was calculated for each section. Size distribution of P2X3r- and TRPV1-positive cells was plotted using R.

2.12. Ca²⁺-imaging analysis

Neurons were identified morphologically, and ROIs were drawn around them for each coverslip using Fiji/ImageJ (National Institute of Health). Background fluorescence was subtracted from fluorescent intensities of ROIs. Baseline fluorescence was calculated by taking the average fluorescence of 20 s before the application of the first stimulus in each experiment, and background- and baseline-subtracted fluorescence (F) was calculated for all neurons from each coverslip. Maximum fluorescence (F_{max}) was calculated from the baseline- and backgroundsubtracted fluorescent intensity following the application of 50 mM KCl at the end of each experiment. Normalized fluorescence intensity (ΔF / F_{max}) was calculated by dividing the difference between F_{max} and F by F_{max} . Neurons were determined as being $\alpha\beta$ -meATP/KCL- responsive if the average $\Delta F/F_{max}$ at pulses were above 0.05 noise threshold (determined from control data) of the baseline. Cells that did not respond to KCl or had an unstable baseline, were excluded from analysis. The peak of each pulse was calculated as the max within the time period of response duration. Proportions of cells responding to different stimuli were calculated using Excel. The peak data were plotted in GraphPad Prism. The size distribution of all neurons analyzed was plotted using the ggplot2 package of R.

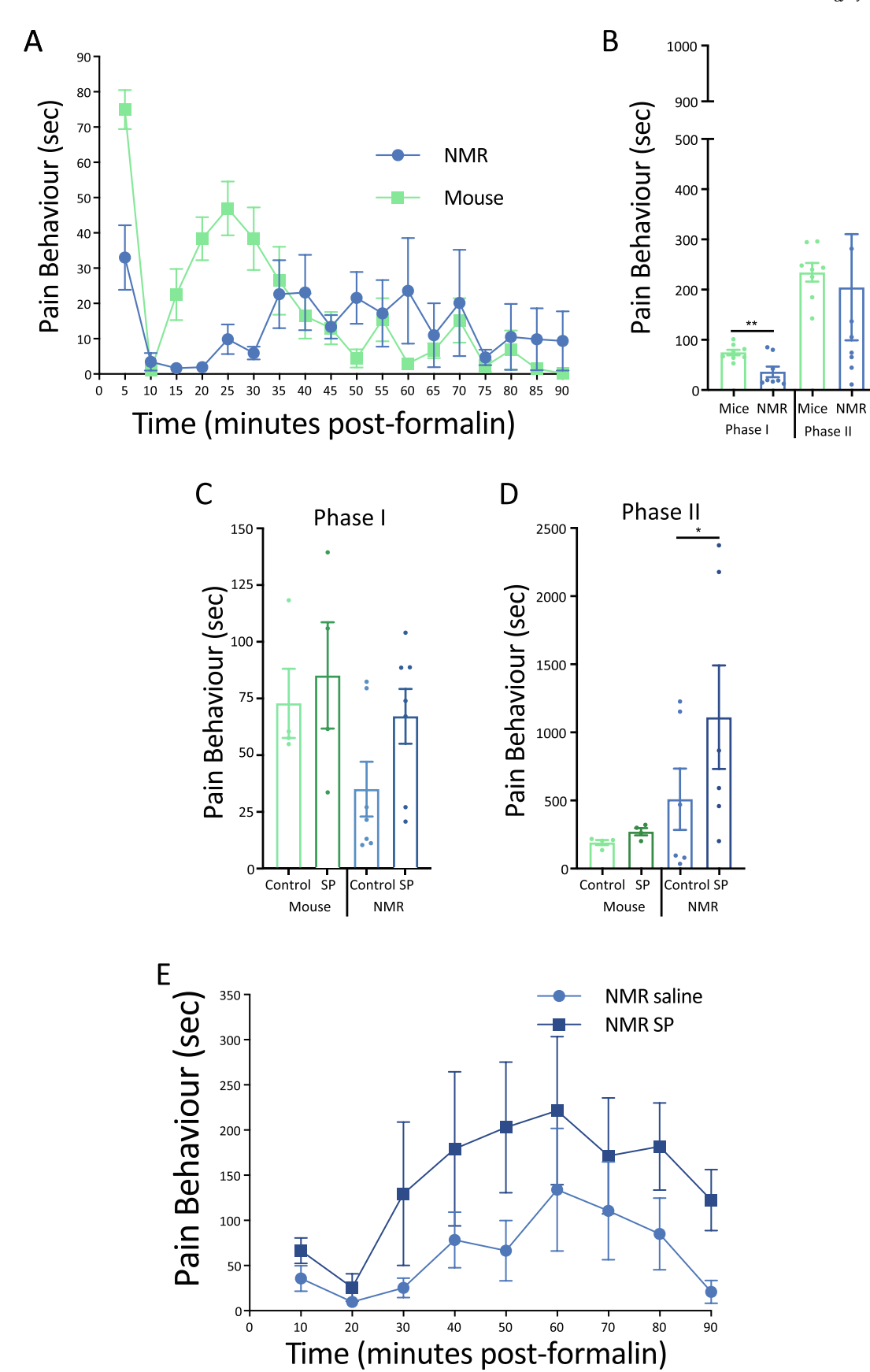
2.13. Statistics

Statistical analysis was carried out using GraphPad Prism version 4 (GraphPad Software, San Diego, CA) or Microsoft Excel. Data from Ca²⁺-imaging, and immunohistochemistry experiments were analyzed and plotted using R and Python. Statistical tests used are referred to where appropriate.

3. Results

As shown in previous studies (Park et al., 2008, Dulu et al., 2014), we found that naked mole-rats show a less intense and longer lasting response to formalin compared to mice (Fig. 1A). However, in the present study, summing the total response times for Phase I (0–10 min) and Phase II (10–90 min), only Phase I showed a significant reduction in response time for naked mole-rats (n = 8) compared to mice (n = 8; p < 0.01; Fig. 1B).

Naked mole-rats lack neuropeptides associated with the peptidergic pain pathway (Park et al., 2003, 2008) and reintroduction of SP can "rescue" capsaicin and histamine sensitivity, as well as sensitizing foot withdrawal to heat (Park et al., 2008; Smith et al., 2010). Therefore, we first examined whether or not introduction of SP via intrathecal injection would affect responses in the formalin test. We observed that SP increased the duration of pain behaviors in both Phase I and Phase II (Fig. 1C, D) of the formalin test in naked mole-rats, such that the duration of responses in Phase I for naked mole-rats was no longer significantly different from that of mice (Fig. 1C). However, in this particular experiment, Phase I control responses to formalin (i.e. without SP) were also not significantly different between mice (n = 4) and naked mole-rats (n = 6). Nevertheless, the duration of responses in Phase II for the naked mole-rats treated with SP was significantly greater compared to both control mice and control naked mole-rat



(caption on next page)

Fig. 1. Naked Mole-Rat and Mouse Response to the Irritant Formalin. Quantification of pain behaviors in mice and naked mole-rats during the formalin test, and the effects of intrathecal (IT) injection of SP. A) Time spent performing pain behaviors (licking, biting, and lifting the formalin-injected foot) as a function of time. Data is shown in 5-minute increments. (n=8 mice and NMR). B) The data are re-plotted and displayed as cumulative time to facilitate species comparisons within Phase I and Phase II. Phase I corresponds to the first 10 min after formalin application. Phase II corresponds to 10–90 min after formalin injection. Here, time of pain behaviors for phase II is summed for the entire 10–90-minute phase (note that all other Phase II data presented for mice correspond to 10–60 min as we did not observe robust pain behaviors after 60 min). C) Time spent in pain behaviors for Phase I of the formalin test after intrathecal injection of SP or saline control. (n=4 mice, n=7 NMR) D) Time spent in pain behaviors for Phase II after intrathecal injection of SP or saline control (same animals as C). E) Quantification of pain behaviors from formalin application following IT injection of SP or saline in naked mole-rats, displayed in 10-minute increments. NMR = naked mole-rat. SP = Substance P. (* p < .05, ** p < .05, ** p < .01, Statistical analysis was performed using a paired T-test).

(p < 0.05; Fig. 1D). SP had no significant effect on Phase I or Phase II in mice, which naturally produce SP in cutaneous nerves. While no individual time point provided a statistically significant change, the significant increase in Fig. 1D can be seen in moderate levels of pain increase during the 10–60-minute range (Fig. 1E), exhibiting a greater intensity in the earlier part of Phase II compared to control naked molerats. Thus, administration of SP enhances formalin-induced pain in naked mole-rats, but not in mice.

Next, we focused on the involvement of P2X3r in formalin-induced pain in naked mole-rats and mice. Prior to applying formalin, we injected one foot with the P2X3r antagonist, A-317491. Ten minutes later, we injected the same foot with formalin. For mice (n = 4), we found no significant effect with the P2X3r antagonist in either Phase I or Phase II response (Fig. 2A, B). However, for naked mole-rats (n = 5), we found that pretreatment with the P2X3r antagonist resulted in a significant reduction in Phase I pain responses (p < .05; Fig. 2A); a reduction of 46% compared to control. The Phase II response was inhibited by an even greater extent of 70% (p < .001; Fig. 2B). These results suggest that a substantial portion of Phase I pain and the majority of Phase II pain is mediated by P2X3r $^+$ (i.e. non-peptidergic) nerves in naked mole-rats.

The species differences in the ability of the P2X3r antagonist to inhibit formalin-induced nocifensive behaviors in mice and naked mole-rats could suggest dissimilar patterns of P2X3r expression in sensory neurons from these species, e.g. greater expression of P2X3r in naked mole-rat DRG neurons. We thus assessed the expression of P2X3r

and TRPV1 in DRG neurons from naked mole-rats and mice (Fig. 3A-E). Consistent with our previous findings (Park et al., 2008; Smith et al., 2012), mice had a more pronounced peak in the number of small diameter neurons (Fig. 3A, B, average cell 358.4 \pm 237.5 μ m²) than naked mole-rats (Fig. 3C, D, average cell 547.3 \pm 295.2 μ m²). However, the proportion of P2X3r⁺ only, TRPV1⁺ only and P2X3r⁺/ TRPV1 + co-expressing neurons was similar between naked mole-rats and mice (Fig. 3B, D naked mole-rat vs. mouse: P2X3r+ only $17.5 \pm 4.8\%$ vs. $28.1 \pm 7.6\%$, TRPV1 + only 24.5 ± 4.8 vs. 15.8 \pm 3.3% and P2X3r⁺/TRPV1⁺ co-expression 11.3 \pm 5.4 vs. $16.5 \pm 0.8\%$). Importantly, the total percentage of P2X3r⁺ neurons was also similar between species (mouse 44.5 ± 8.2% vs. naked molerat 28.8 ± 5.9%, Fig. 3E) and consistent with this result, in a functional Ca2+-imaging assay, we observed that the proportion of DRG neurons responding to the P2X3r agonist, α-β-met-ATP was not significantly different between species (Fig. 3F, naked mole-rat $42.9 \pm 9.6\%$ and mouse $55.3 \pm 2.9\%$). Given these results, we interpret the in vivo species differences to the antagonist in Fig. 2 to be due to species differences in the peptidergic pathway. For example, it is possible that, for mice, the effects of antagonizing the purinergic pathway are masked by simultaneously activating the peptidergic pathway, which would not be the case for the naked mole-rat.

We next turned our attention to the endocannabinoid system and how it interacts with the purinergic pathway. To make that assessment, we pre-treated animals with an IP injection of the non-selective CB1r agonist, WIN55, or saline (control). Thirty minutes later, we injected

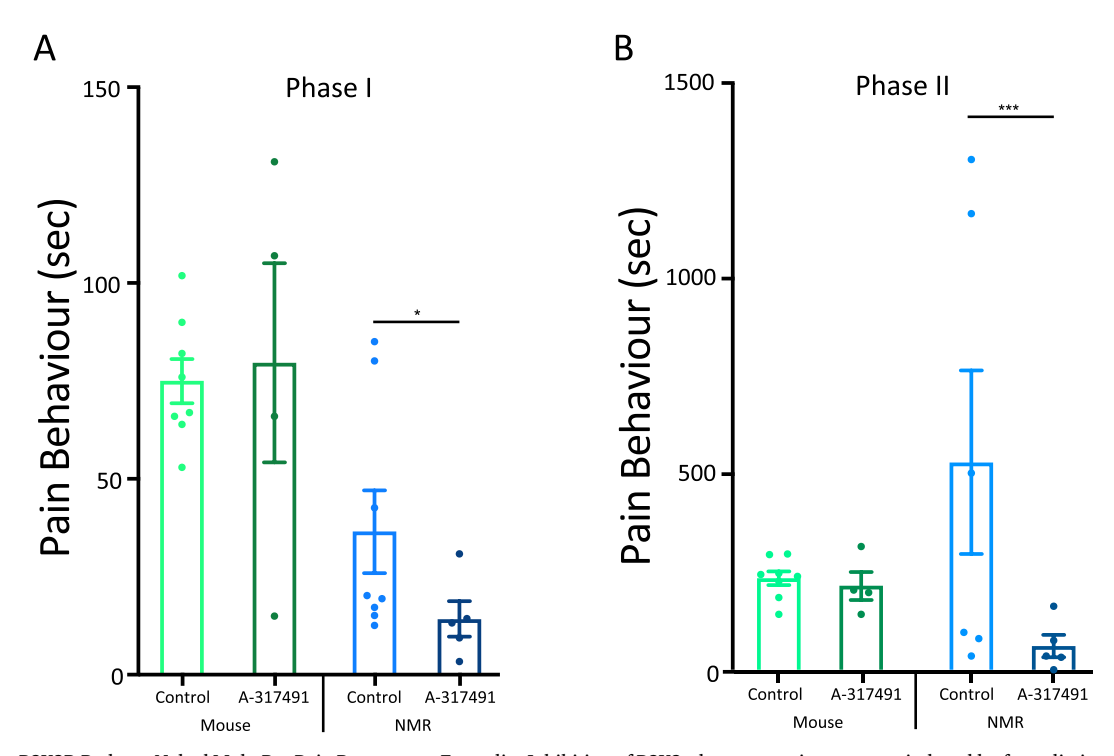


Fig. 2. Inhibiting P2X3R Reduces Naked Mole-Rat Pain Response to Formalin. Inhibition of P2X3r decreases pain responses induced by formalin in naked mole-rats in Phase I (A) and Phase II (B) but has no effect on those responses in mice. P2X3r Ant = Antagonist A-317491. (n = 8 mice and NMR saline control; 4 mice and 5 NMR with antagonist; * p < .05, *** p < .05, *** p < .001, Statistical analysis was performed using a paired T-test).

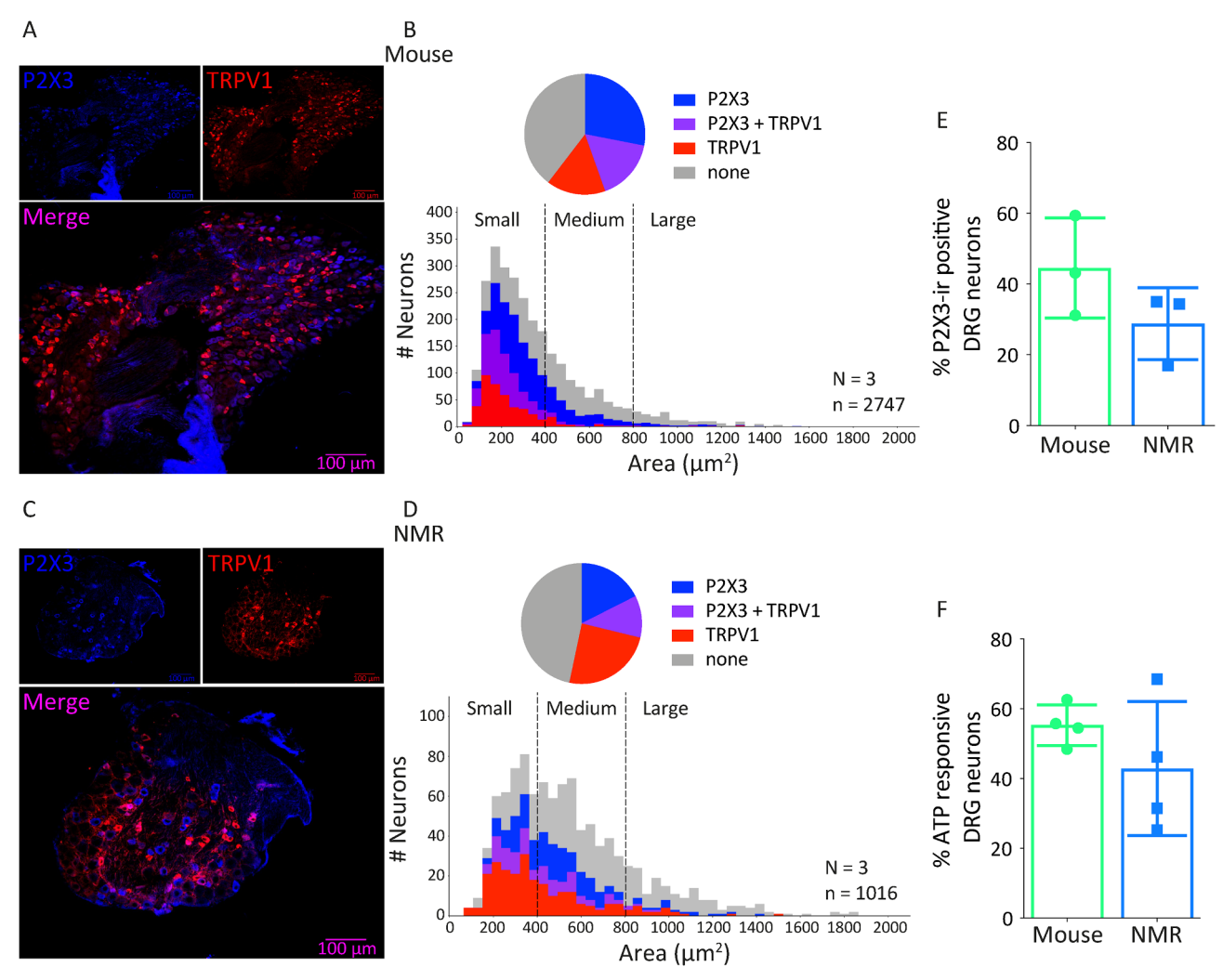


Fig. 3. P2X3R is Functional in Cultured Naked Mole-Rat Dorsal Root Ganglion Neurons. Functionality of P2X3r was assessed with IHC and Ca^{2+} -imaging. Example images of P2X3r and TRPV1 expression in DRG neurons of mice (A, n = 3) and naked mole-rats (C, n = 3). Quantification of neurons by cell area in mice (B) and naked mole-rats (D) shows a similar distribution of P2X3r and TRPV1 expression/co-expression but note the enhanced peak of small diameter fibers in mouse compared to naked mole-rat. Quantification of P2X3r expression in mouse and naked mole-rat DRG reveals no significant difference (E, n = 3). Responsiveness of mouse and naked mole-rat DRG neurons to the P2X3r agonist αβ-meATP is similar across species (F, n = 4). Statistical analysis of data in E and F was performed using Mann Whitney U test.

one foot with the P2X3r agonist, α - β -met-ATP (ATP). Ten minutes later, we performed the von Frey assay of mechanical pain sensitivity on both the ATP-injected paw (ipsilateral) and the non-injected paw (contralateral). This test, 10 min after ATP application, was intended to assess the short-term effects of ATP sensitization on mechanical sensitivity. We tested both paws again 180 min after the ATP injection to assess the inflammatory response. In control naked mole-rats (n = 6), the paw withdrawal threshold 10 min after ATP injection showed a significantly lower threshold than the contralateral paw, indicating sensitization of the ipsilateral paw due to ATP treatment (Fig. 4A). Pretreatment with WIN55 produced a significantly higher ipsilateral threshold compared to saline treated animals (Fig. 4A) and the threshold was not significantly different to the contralateral paw threshold (Fig. 4A). Thus, the data indicate that activation of CB1r inhibits the function of the purinergic pathway in naked mole-rats. WIN55 did not significantly change the paw withdrawal threshold for the paw that was not injected with ATP (Fig. 4A).

We tested for a long-term (inflammatory) response from ATP activation of P2X3r by reassessing animals at 180 min post ATP application. However, ATP did not cause any long-term sensitization in naked mole-rats and WIN55 also had no effect on the paw withdrawal threshold (p > .05; Fig. 4A).

In mice (n = 7), ATP alone caused significant sensitization (Fig. 4B), similar to that observed in naked mole-rats. However, the dose of WIN55 that reduced naked mole-rat ATP-induced sensitization did not attenuate sensitization in mice at 10 min post ATP application (Fig. 4B). Regarding long-term effects of ATP, the average threshold of the ATP injected paw was lower than the average threshold of the contralateral paw, but the difference was not significant (Fig. 4B). There was, however, a significant sensitization response in mice at 180 min post ATP after pretreatment with WIN55 (Fig. 4B). Given that this dose of WIN55 did not attenuate pain in the 10 min mouse group, we interpret the sensitization in the 180 min mouse group to be the result of inflammation from the ATP.

The von Frey experiment showed that stimulating CB1r signaling attenuated P2X3r-dependent sensitization to acute mechanical stimulation in the naked mole-rats but not the mice. Next, we tested the effects of stimulating CB1r in the formalin test. The CB1r agonist WIN55 significantly reduced Phase I pain behaviors in mice (n=8), but not in naked mole-rats (n=8; Fig. 5A), suggesting perhaps that CB1r signaling may reduce acute chemical pain (Phase I) via the peptidergic pain pathway, which is functional in mice, but non-functional in naked mole-rats. The results were different in the inflammatory phase of the formalin test (Phase II), such that in both mice and naked mole-rats

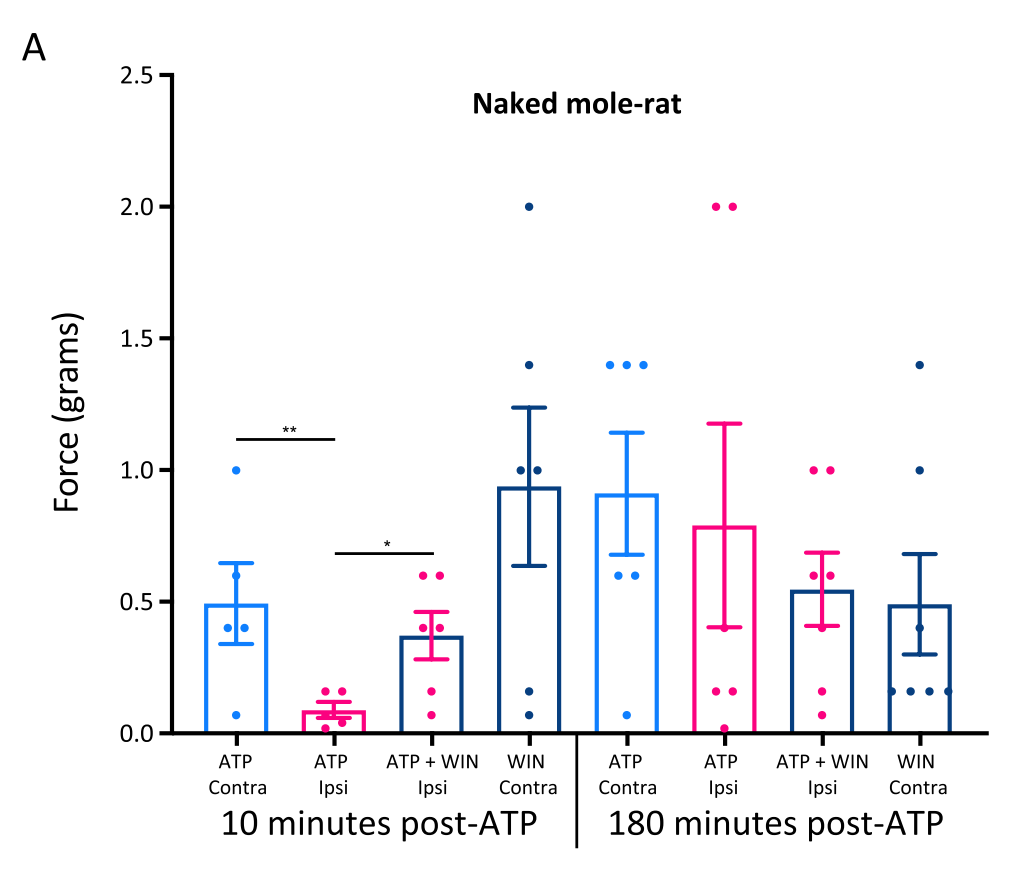
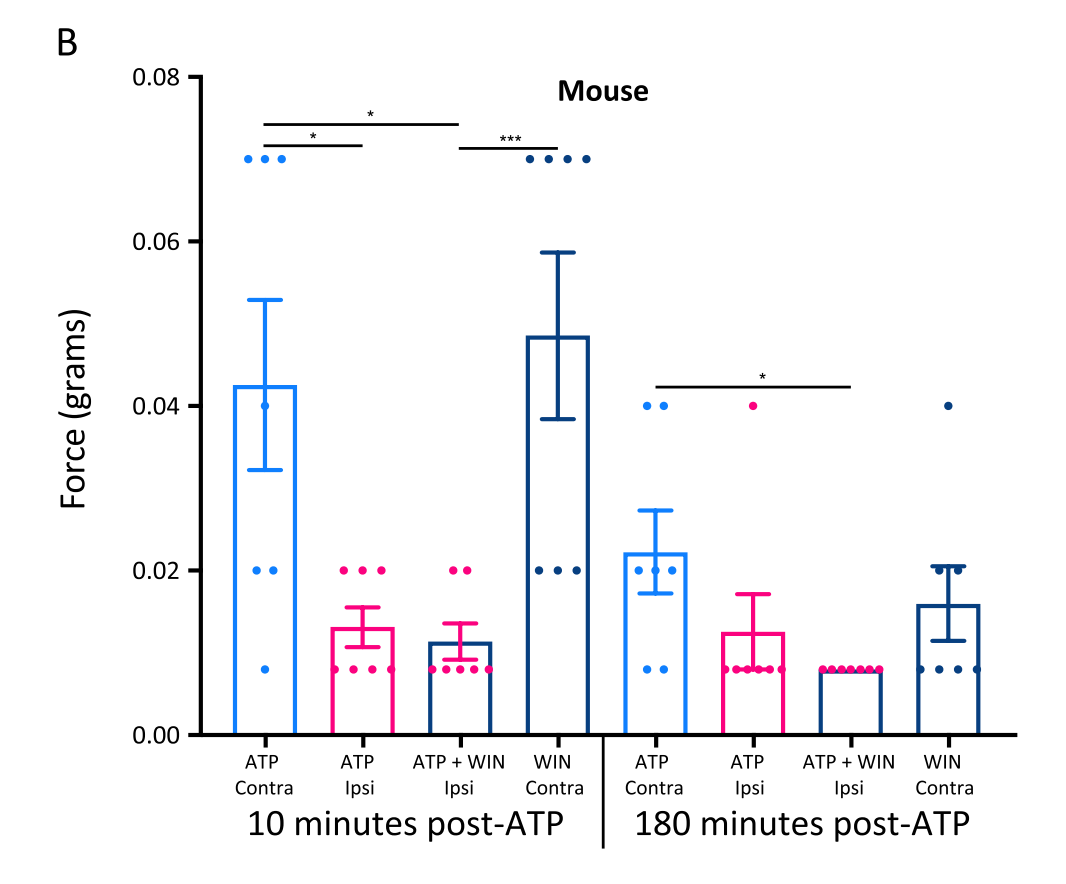


Fig. 4. Mechanical Pain Response to ATP in Naked Mole-Rats and Mice. Naked mole-rat and mouse response to von Frey stimuli following application of 5 μ g α - β -met-ATP (ATP) to the plantar surface of the hind paw. A) Data from naked mole-rats. The first four bars show data collected 10 min after ATP application to one paw. The first two bars show the thresholds for paw withdrawal from pressure after pretreatment with IT saline. 30 min after IT pretreatment, the plantar surface of one paw was injected with 5 µg ATP. The first bar shows the threshold for the uninjected paw (Contra). The second bar shows the threshold for the paw injected with ATP, which shows significant sensitization (ATP IPSI). The third and fourth bars show thresholds after pretreatment with IT injection of 0.3 mg/kg of the CB1r agonist WIN55. The third bar shows that WIN55 decreases sensitization from ATP (ATP + WIN55 IPSI). The fourth bar shows the threshold for the paw not injected with ATP after pretreatment with WIN55. The last four bars repeat these conditions, but the data were collected 180 min after ATP application instead of 10 min. B) Data from mice, the bars are associated with the same conditions described above for (A). (n = 6NMR, 7 mice; *p < .05, *** p < .01, *** p < .001, Statistical analysis was performed using a 2way- ANOVA with Tukey post-Hoc analysis).



WIN55 produced a significant reduction in pain behaviors (Fig. 5B). These results suggest a robust influence of CB1r signaling on the purinergic pain pathway in inflammatory pain in both species, i.e. an effect

that is presumably independent of peptidergic neurons due to lack of neuropeptides in the C-fibers of naked mole-rat.

Stimulating CB1r signaling can have a wide range of effects in

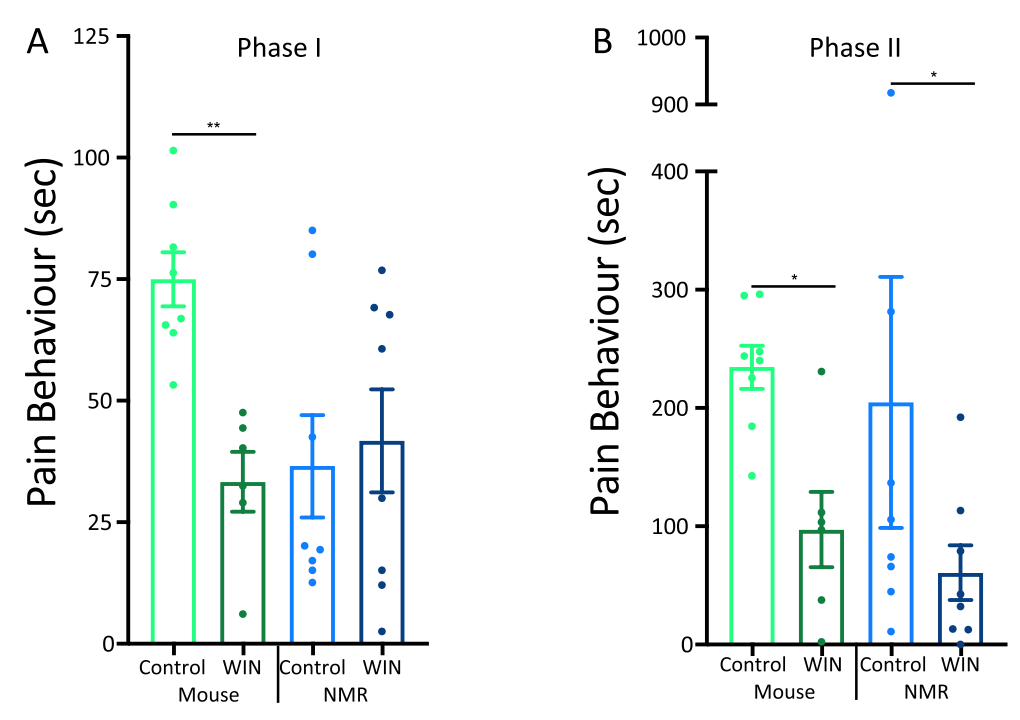


Fig. 5. WIN55 Attenuates Pain in Phase II of the Formalin Test. The CB1r agonist WIN55 (3 mg/kg) attenuates the behavioral responses induced by formalin in both Phase I (A) and Phase II (B) for mice, but only Phase II for naked mole-rats. (n = 8; * p < 0.05, ** p < 0.01, Statistical analysis was performed using a paired T-test).

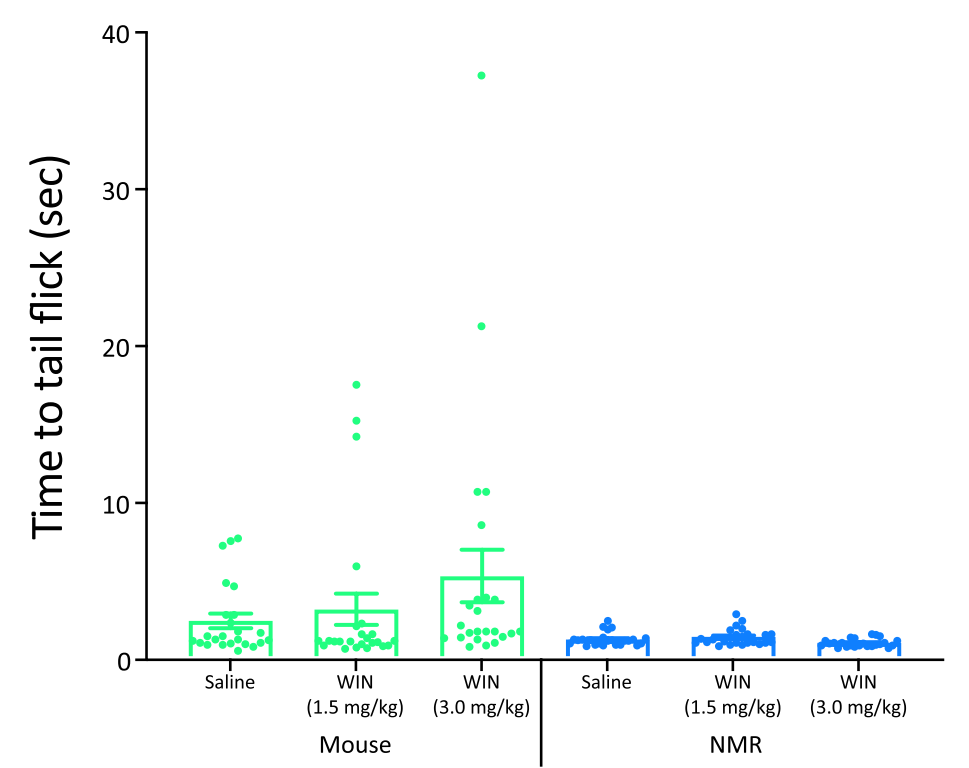


Fig. 6. WIN55 Does Not Reduce Thermal Pain. Thermal pain was assessed by immersion of the animal's tail into water at 48 °C and recording the latency to tail flick. Naked mole-rats response latencies with control, 1.5 mg/kg WIN55, and 3 mg/kg WIN55 were compared as were mice responses at the same doses and no significant differences were observed in either species. (n = 24 mice and NMR; * p < .05, Statistical analysis was performed using a 1way-ANOVA with Tukey post-Hoc analysis).

addition to relieving inflammatory pain (Elphick and Egertova, 2001). For example, CB1r agonists can slow motor responses. To support the hypothesis that the WIN55 effect observed in the inflammatory phase of the formalin test was due to CB1r signaling in P2X3r⁺ fibers, we assessed the response of WIN55 on acute thermal pain, which is thought to be independent of P2X3r⁺ fibers (Ramer et al., 2001; Souslova et al., 2000). We previously showed that naïve naked mole-rats have a normal (mouse-like) response to acute thermal pain in a foot withdrawal to

radiant heat procedure (Park et al, 2008). In the current study, we employed the tail flick test and observed that the time to tail flick after emersion in 48 °C water was not significantly reduced after pretreatment with WIN55 in either naked mole-rats or mice, compared to pretreatment with saline (n = 24; Fig. 6). This result suggests that the reduction in inflammatory pain we observed in the formalin test was due to CB1r agonist-induced analgesia and not induction of sedation/hypomobility. Note that the mice showed a non-significant trend

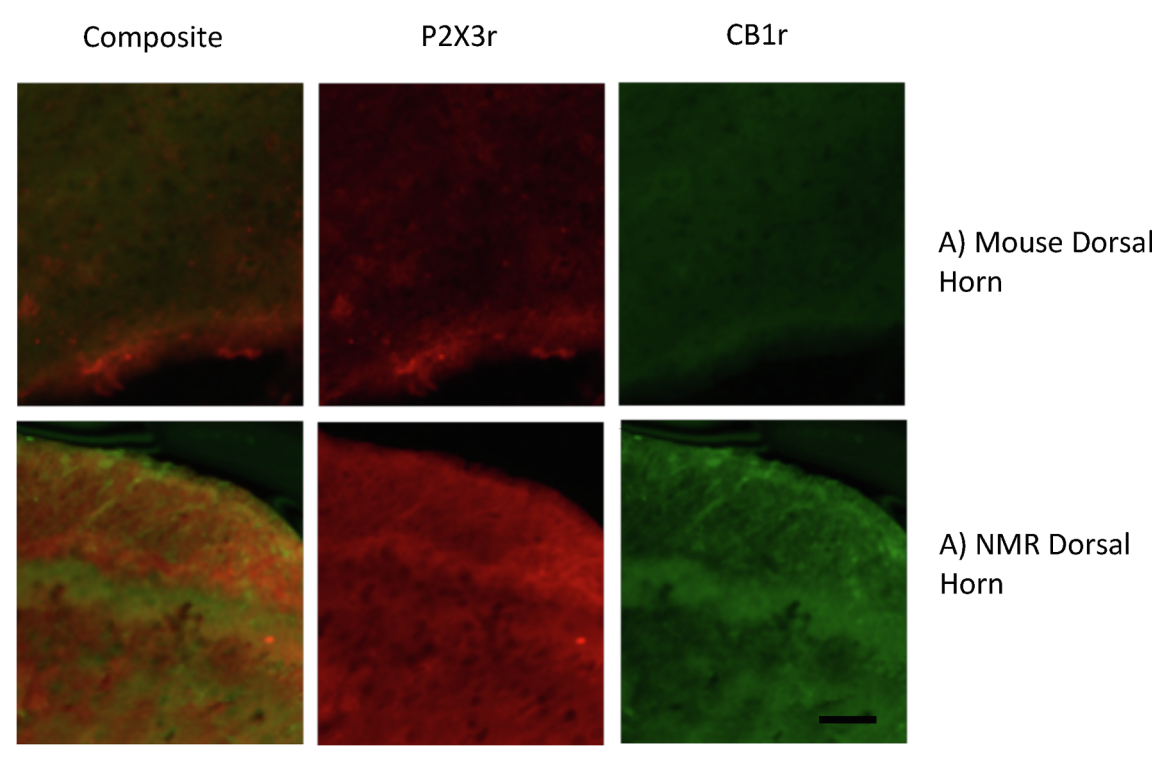


Fig. 7. CB1r and P2X3r are Co-expressed in Lamina II of the Dorsal Horn of Mice and Naked Mole-Rat Spinal Cords Example confocal images of CB1r and P2X3r expression in the dorsal horn of the spinal cord in mice (A) and naked mole-rats (B). Scale bar 25 μm.

toward an increase in latency (all mouse data ANOVA: p=.2; control vs. 3 mg/kg, t-test: p=.11), which may have been due to a hypomobility response from the WIN55, which was not apparent in naked molerats.

Finally, we used immunochemistry to examine the overlap of CB1r and P2X3r in lamina II of the dorsal horn where P2X3r+ fibers terminate and where CB1r activation may mediate its effect (Fig. 7). Both species expressed CB1r and P2X3r in a similar manner. We analyzed the proximity of CB1r to P2X3r to determine if there was colocalization between the receptors. We found no significant difference between overlap in mice (n = 3; Fig. 7A; 0.95 \pm 0.007) compared to naked mole-rats (n = 8; Fig. 7B; 0.969 \pm 0.004) though the individual indices for naked mole-rats (Index 1-CB1r: 1.04 ± 0.13; Index2- P2X3r: 0.977 ± 0.14) were closer to a 1:1 ratio than that of mice (Index 1-CB1r: 0.745 \pm 0.05; Index2- P2X3r: 1.24 \pm 0.07). Individual Pearson Coefficients were also calculated for each dorsal horn imaged. In naked mole-rats, the coefficients all showed at least a moderately positive correlation with a range from 0.37 to 0.81. The percentage of images with a relatively strong positive correlation (> 0.5) were 69.23% and with a strong positive correlation was 38.46% (n = 13). The range of Pearson coefficients in mice was from 0.32 to 0.88, i.e. greater variation than in naked mole-rats. There were also fewer images that were in the relatively strong (42.85%) and strong (14.28%) correlation ranges.

4. Discussion

This study aimed to determine the functionality of non-peptidergic P2X3r⁺ fibers, the role of P2X3r in inflammatory pain, and modulation of nociception by CB1r signaling in naked mole-rats. Binding of the non-peptidergic neuron marker IB4 has been shown to be similar in naked mole-rats and mice with regard to the proportion of DRG neurons labelled and afferent terminals in the dorsal horn of the spinal cord (Park et al., 2008). By contrast, naked mole-rats lack neuropeptide signaling in cutaneous C-fibers (Park et al., 2003, 2008). However, the purinergic pathway had not previously been examined.

Naked mole-rats have a diminished response to formalin compared

to mice (Park et al., 2008; Fig. 1) and here we showed that intrathecal SP administration enhanced the formalin-induced pain response in naked mole-rats, suggesting that activation of the peptidergic pathway is important for the full behavioral response and that the pain behaviors observed without intrathecal SP are likely mediated by non-peptidergic fibers. Indeed, administration of the P2X3r antagonist A-317491 significantly reduced both phases of the formalin response in naked molerats, but not in mice (Fig. 2). This species difference in behavioral response cannot be explained by a difference in proportion of DRG neurons in mouse and naked mole-rat that express P2X3r, as shown through both immunohistochemistry and Ca2+-imaging (Fig. 3). Further evidence of a fully functional purinergic pain pathway in naked mole-rats is that, similar to mice, the naked mole-rats show mechanical hypersensitivity following administration of the P2X3r agonist ATP (Fig. 4). Interestingly, we observed no sensitization effect of ATP on naked mole-rats 180 min after ATP application. Our data and previous studies in mice have indicated that the 3-hour time point was indicative of an inflammatory response, and mice were more sensitive during that time than at earlier time points (Oliveira-Fusaro et al., 2017). This observation raises the possibility that the peptidergic pathway may be necessary to stimulate the ATP-dependent inflammatory response.

Considering the growing interest in cannabinoid-based therapeutics and the evidence from studies in mice and rats that activation of CB1r results in analgesia, we explored the functionality of the cannabinoid system in naked mole-rats, the first study to investigate this system in this species to our knowledge. Whereas in mice, application of the CB1r agonist WIN55 caused a significant reduction in pain behaviors in both Phases I and Phase II of the formalin response, only the inflammatory phase (Phase II) was reduced in naked mole-rats (Fig. 5). Because the CB1r agonist was able to reduce pain in naked mole-rats, which lack endogenous neuropeptide signaling in cutaneous C-fibers, this result suggests that the cannabinoid system likely reduces inflammatory pain exclusively through non-peptidergic, P2X3r⁺ neurons in naked mole-rats. The lack of analgesia produced by WIN55 in naked mole-rats in the acute Phase (Phase I; Fig. 5A), suggests a greater role for activation of peptidergic neurons in Phase I and indeed formalin has been shown to

activate TRPA1 and produce nocifensive behaviors in a TRPA1-dependent manner, moreover, some, but not all, studies have shown greater expression of TRPA1 in peptidergic compared to non-peptidergic neurons in mice (McNamara et al., 2007; Hockley et al., 2019; Zeisel et al., 2018); although naked mole-rats respond behaviorally to TRPA1 agonists (Eigenbrod et al., 2019), the expression profile of TRPA1 in naked mole-rat DRG neurons remains unknown.

We wish to point out a cautionary issue to be considered. The concentration of formalin that we used (2%) has previously been shown to induce long-term behavioral hypersensitivity (at least 14 days) and enhanced expression of activating transcription factor 3 (ATF3) in DRG neurons, both of which are indicative of nerve injury (Bráz and Basbaum, 2010; Salinas-Abarca et al., 2017; Tsujino et al., 2000). Nerve injury can cause neuronal activity in a heterogeneous population of sensory neurons. Thus, our behavioral data may reflect, to some extent, activity in neurons other than purinergic C-fibers, namely A-delta fibers. However, we do not believe that this caveat detracts from the significant effects that we found from agonizing and antagonizing purinergic receptors.

Overall, we found that naked mole-rat non-peptidergic, P2X3r⁺ C-fibers are able to functionally receive and relay nociceptive signals. Additionally, activation of CB1r is able to reduce inflammatory pain signaling in naked mole-rats. Taken together, our results suggest that the naked mole-rat may be a useful model for studying features of the purinergic pain pathway in the absence of a functional peptidergic pain pathway.

CRediT authorship contribution statement

Brigitte M. Browe: Conceptualization, Formal analysis, Writing original draft, Methodology, Investigation. Abigail R. Olsen: Investigation. Cesar Ramirez: Investigation. Rebecca H. Rickman: Formal analysis, Investigation. Ewan St. John Smith: Conceptualization, Formal analysis, Writing - review & editing, Methodology, Supervision. Thomas J. Park: Conceptualization, Writing - review & editing, Investigation, Methodology, Supervision.

Declaration of Competing Interest

The authors declare that they have no known competing financial interests or personal relationships that could have appeared to influence the work reported in this paper.

Acknowledgements

This work has been supported by the following: a grant from the National Science Foundation (1655494) and a UIC LAS Award for Faculty of Sciences to T.J.P., and a CRUK Grant (C56829/A22053) to ESS. We are grateful to Mr. Symmorron Bailey for excellent animal care.

References

- Agarwal, N., Pacher, P., Tegeder, I., Amaya, F., Constantin, C.E., Brenner, G.J., Rubino, T., Michalski, C.W., Marsicano, G., Monory, K., Mackie, K., Marian, C., Batkai, S., Parolaro, D., Fischer, M.J., Reep, P., Kunos, G., Kress, M., Lutz, B., Woolf, C.J., Kuner, R., 2007. Cannabinoids mediate analgesia largely via peripheral type 1 cannabinoid receptors in nociceptors. Nat. Neurosci. 10 (7), 870–879. https://doi.org/10.1038/nn1916.
- Amaya, F., Shimosato, G., Kawasaki, Y., Hashimoto, S., Tanaka, Y., Ji, R.R., Tanaka, M., 2006. Induction of CB1 cannabinoid receptor by inflammation in primary afferent neurons facilitates antihyperalgesic effect of peripheral CB1 agonists. Pain 124, 175–183. https://doi.org/10.1016/j.pain.2006.04.001.
- Artwohl, J., Hill, T., Comer, C.M., Park, T.J., 2002. Naked mole-rats: unique opportunities and husbandry challenges. Laboratory Anim. 31, 32–36. https://doi.org/10.1038/5000156.
- Brand, A., Smith, E.S.J., Lewin, G.R., Park, T.J., 2010. Functional neurokinin and NMDA receptor activity in an animal naturally lacking substance P: the naked mole-rat. PLoS One 5 (12), e15162. https://doi.org/10.1371/journal.pone.0015162.
- Bráz, J.M., Basbaum, A.I., 2010. Differential ATF3 expression in dorsal root ganglion

- neurons reveals the profile of primary afferents engaged by diverse noxious chemical stimuli. Pain 150 (2), 290–301. https://doi.org/10.1016/j.pain.2010.05.005.
- Calignano, A., La Rana, G., Giuffrida, A., Piomelli, D., 1998. Control of pain initiation by endogenous cannabinoids. Nature 394 (6690), 277–281. https://doi.org/10.1038/ 28393
- Carey, L.M., Slivicki, R.A., Leishman, E., Cornett, B., Mackie, K., Bradshaw, H., Hohmann, A.G., 2016. A pro-nociceptive phenotype unmasked in mice lacking fatty-acid amide hydrolase. Mol. Pain 13 (12). https://doi.org/10.1177/1744806916649192.
- Cauwels, A., Rogge, E., Vandendriessche, B., Shiva, S., Brouckaert, P., 2014. Extracellular ATP drives systemic inflammation, tissue damage, and mortality. Cell Death Dis. 5, e1102. https://doi.org/10.1038/cddis.2014.70.
- Cavanaugh, D.J., Chesler, A.T., Braz, J.M., Shah, N.M., Julius, D., Basbaum, A.I., 2011. Restriction o transient receptor potential vanilloid-1 to the peptidergic subset of primary afferent neurons follows its developmental downregulation in nonpeptidergic neurons. J. Neurosci. 31 (28), 10119–10127. https://doi.org/10.1523/ JNEUROSCI.1299-11.2011.
- Chaplan, S.R., Bach, F.W., Pogrel, J.W., Chung, J.M., Yaksh, T.L., 1994. Quantitative assessment of tactile allodynia in the rat paw. J. Neurosci. Methods 53 (1), 55–63. https://doi.org/10.1016/0165-0270(94)90144-9.
- Chiou, L., Hu, S.S., Ho, Y., 2013. Targeting the cannabinoid system for pain relief? Acta Anaesthesiol. Taiwanica 51 (4), 161–170. https://doi.org/10.1016/j.aat.2013.10.
- Coderre, T.J., Katz, J., Vaccarino, A.L., Melzack, R., 1993. Contribution of central neuroplasticity to pathological pain: review of clinical and experimental evidence. Pain 52 (3), 259–285. https://doi.org/10.1016/0304-3959(93)90161-h.
- Dickenson, A.H., Sullivan, A.F., 1987. Peripheral origins and central modulation of subcutaneous formalin-induced activity of rat dorsal horn neurones. Neurosci. Lett. 83 (1–2), 207–211. https://doi.org/10.1016/0304-3940(87)90242-4.
- Dulu, T.D., Kanui, T.I., Towett, P.K., Maloiy, G.M., Abelson, K.S.P., 2014. The effects of oxotremorine, epibatidine, atropine, mecamylamine and naloxone in the tail-flick, hot-plate, and formalin tests in the naked mole-rat (*Heterocephalus glaber*). Vivo 28 (1), 39–48. http://iv.iiarjournals.org/content/28/1/39.long.
- Eberhardt, M., Stueber, T., de la Roche, J., Herzog, C., Leffler, A., Reeh, P.W., Kistner, K., 2017. TRPA1 and TRV1 are required for lidocaine-evoked calcium influx and neuropeptide release but not cytotoxicity in mouse sensory neurons. PLoS One 12 (11), e0188008. https://doi.org/10.1371/journal.pone.0188008.
- Eigenbrod, O., Debus, K.Y., Reznick, J., Bennett, N.C., Omerbašić, D., Sánchez-Carranza, O., Hart, D.W., Barker, A.J., Lutermann, H., Katandukila, J.V., Mgode, G., Park, T.J., Lewin, G.R., 2019. Rapid molecular evolution of pain insensitivity in multiple African rodents. Science 364, 852–859. https://doi.org/10.1126/science.aau0236.
- Elphick, M.R., Egertova, M., 2001. The neurobiology and evolution of cannabinoid signalling. Philos. Trans. R. Soc. Lond. B Biol. Sci. 356 (1407), 381–408. https://doi.org/10.1098/rstb.2000.0787.
- Evans, R.M., Scott, R.H., Ross, R.A., 2004. Multiple actions of anandamide on neonatal rat cultured sensory neurons. Br. J. Pharmacol. 141, 1223–1233. https://doi.org/10.1038/si.bip.0705723.
- Herkenham, M., Lynn, A.B., Johnson, M.R., Melvis, L.S., de Costa, B.R., Rice, K.C., 1991. Characterization and localization of cannabinoid receptors in rat brain: a quantitative in vitro autoradiographic study. J. Neurosci. 11, 563–583. https://doi.org/10.1523/ JNEUROSCI.11-02-00563.1991.
- Hockley, J.R.F., Taylor, T.S., Gallejo, G., Willbrey, A.L., Gutteridge, A., Bach, K., Winchester, W.J., Bulmer, D.C., McMurray, G., Smith, E.S.J., 2019. Single-cell RNAseq reveals seven classes of colonic sensory neuron. Neurogastroenterology 68, 633–644. https://doi.org/10.1136/gutjnl-2017-315631.
- Hohmann, A.G., Tsou, K., Walker, J.M., 1999. Intrathecal cannabinoid administration suppresses noxious stimulus-evoked Fos protein-like immunoreactivity in rat spinal cord: comparison with morphine. Zhongguo Yao Li Xue Bao 20, 1132–1136. http:// www.chinaphar.com/article/view/8351/8993.
- Hunskaar, S., Hole, K., 1987. The formalin test in mice: dissociation between inflammatory and non-inflammatory pain. Pain 30 (1), 103–114. https://doi.org/10. 1016/0304-3959(87)90088-1.
- Kreitzer, A.C., Regehr, W.G., 2002. Retrograde signaling by endocannabinoids. Curr. Opin. Neurobiol. 12 (3), 324–330. https://doi.org/10.1038/28393.
- LaVinka, P.C., Park, T.J., 2012. Blunted behavioral and C Fos responses to acidic fumes in the African naked mole-rat. PLoS One 7 (9). https://doi.org/10.1371/journal.pone. 0045060. e45060.
- Ma, X., Zhang, F., Dong, F., Bao, L., Zhang, X., 2015. Experimental evidence for alleviating nociceptive hypersensitivity by single application of capsaicin. Mol. Pain, i 11. https://doi.org/10.1186/s12990-015-0019-0.
- Martin, W.J., Patrick, S.L., Coffin, P.O., Tsou, K., Walker, J.M., 1995. An examination of the central sites of action of cannabinoid-induced antinociception in the rat. Life Sci. 56, 103–109. https://doi.org/10.1016/0024-3205(95)00195-c.
- Martin, W.J., Hohmann, A.G., Walker, J.M., 1996. Suppression of noxious stimulusevoked activity in the ventral posterolateral nucleus of the thalamus by a cannabinoid agonist: correlation between electrophysiological and antinociceptive effects. J. Neurosci. 16, 6601–6611. https://doi.org/10.1523/JNEUROSCI.16-20-06601.1996.
- McNamara, C.R., Mandel-Brehm, J., Bautista, D.M., Siemens, J., Derian, K.L., Zhao, M., Hayward, N.J., Chong, J.A., Julius, D., Moran, M.M., Fanger, C.M., 2007. TRPA1 mediates formalin-induced pain. PNAS 104 (33), 13525–13530. https://doi.org/10. 1073/pnas.0705924104.
- Nackley, A.G., Suplita, R.L., Hohmann, A.G., 2003. A peripheral cannabinoid mechanism suppresses spinal fos protein expression and pain behavior in a rat model of inflammation. Neuroscience 117, 659–670. https://doi.org/10.1016/s0306-4522(02) 00870-9.
- Nerandzic, V., Mrozkova, P., Adamek, P., Spicarova, D., Nagy, I., Palecek, J., 2018.

 Peripheral inflammation affects modulation of nociceptive synaptic transmission in

the spinal cord induced by N-arachidonylphosphatidylethanaloamine. Br. J. Pharmacol. 175 (12), 2322–2336. https://doi.org/10.1111/bph.13849.

- Oliveira, M.C., Pelegrini-da-Silva, A., Tambeli, C.H., Parada, C.A., 2009. Peripheral mechanisms underlying the essential role of P2X3, 2/3 receptors in the development of inflammatory hyperalgesia. Pain 141, 127–134. https://doi.org/10.1016/j.pain. 2008.10.024.
- Oliveira-Fusaro, M.C.G., Zanoni, C.I.S., dos Santos, G.C., Manzo, L.P., Araldi, D., Bonet, I.J.M., et al., 2017. Antihyperalgesic effect of CB1 receptor activation involves the modulation of P2X3 receptor in the primary afferent neuron. Eur. J. Pharmacol. 798, 113–121. https://doi.org/10.1016/j.ejphar.2017.01.030.
- Omerbasic, D., Smith, E.S.J., Moroni, M., Homfeld, J., Eigenbrod, O., Bennet, N.C., Reznick, J., Faulkes, C.G., Selbach, M., Lewin, G.R., 2016. Hypofunctional TrkA accounts for the abscence of pain sensitization in the African naked mole-rat. Cell Rep. 17 (3), 748–758. https://doi.org/10.1016/j.celrep2016.09.035.
- Park, T.J., Comer, C.M., Carol, A., Lu, Y., Hong, H.-S., Rice, F.L., 2003. Somatosensory organization and behavior in naked mole-rats II: peripheral structures, innervation, and selective lack of neuropeptides associated with thermoregulation and pain. J. Comp. Neurol. 465, 104–120. https://doi.org/10.1002/cne.10824.
- Park, T.J., Lu, Y., Jüttner, R., Smith, E.S., Hu, J., Brand, A., Wetzel, C., Milenkovic, N., Erdmann, B., Heppenstall, P.A., Laurito, C.E., Wilson, S.P., Lewin, G.R., 2008. Selective inflammatory pain insensitivity in the African naked mole-rat (Heterocephalus glaber). PLoS Biol. 6 (1), e13. https://doi.org/10.1371/journal.pbio.0060012
- Raboisson, P., Dallel, R., Clavelou, P., Sessle, B.J., Woda, A., 1995. Effects of subcutaneous formalin on the activity of trigeminal brain stem nociceptive neurones in the rat. J. Neurophysiol. 73 (2), 496–505. https://doi.org/10.1152/jn.1995.73.2.496
- Ramer, M.S., Bradbury, E.J., McMahon, S.B., 2001. Nerve growth factor induces P2X(3) expression in sensory neurons. J. Neurochem. 77 (3), 864–875. https://doi.org/10.1046/j.1471-4159.2001.00288.x.
- Rigoni, M., Trevisani, M., Gazzieri, D., Nadaletto, R., Tognetto, M., Creminon, C., Davis, J.B., Campri, B., Amadesi, S., Geppetti, P., Harrison, S., 2009. Neurogenic repsonses mediated by vanilloid receptor-1 (TRPV1) are blocked by the high affinity antagonist, iodo-resiniferatoxin. Br. J. Pharmacol. 138 (5), 977–985. https://doi.org/10.1038/sj.bjp.0705110.
- Salinas-Abarca, A.B., Avila-Rojas, S.H., Barragán-Iglesias, P., Pineda-Farias, J.B., Granados-Soto, V., 2017. Formalin injection produces long-lasting hypersensitivity with characteristics of neuropathic pain. Eur. J. Pharmacol. 15 (797), 83–93. https://doi.org/10.1016/j.eiphar.2017.01.018.
- Shibata, M., Ohkubo, T., Takahashi, H., Inoki, R., 1989. Modified formalin test: characteristic biphasic pain response. Pain 38 (3), 347–352. https://doi.org/10.1016/0304-3959(89)90222-4.
- Smith, E.S.J., Blass, G.R.C., Lewin, G.R., Park, T.J., 2010. Absence of histamine-induced

- itch in the African naked mole-rat and "rescue" by Substance P. Mol. Pain 29. https://doi.org/10.1186/1744-8069-6-29.
- Smith, E.S.J., Omerbasic, D., Lecher, S.G., Anirudhan, G., Lapatsina, L., Lewin, G.R., 2011. The molecular basis of acid insensitivity in the Africa naked mole-rat. Science 334 (6062), 1557–1560. https://doi.org/10.1126/science.1213760.
- Smith, E.S.J., Purfurst, B., Grigoryan, T., Park, T.J., Bennett, N.C., Lewin, G.R., 2012. Specific paucity of unmyelinated C-fibers in cutaneous peripheral nerves of the African naked-mole rat: comparative analysis using six species of bathyergidae. J. Comp. Neurol. 520 (12), 2785–2803. https://doi.org/10.1002/cne.23133.
- Smith, E.S.J., Park, T.J., Lewin, G.R., 2020. Independent evolution of pain insensitivity in African mole-rats: origins and mechanisms. J. Comp. Physiol. A Neuroethol. Sens. Neural Behav. Physiol. https://doi.org/10.1007/s00359-020-01414-w. [Epub ahead of print]
- Souslova, V., Cesare, P., Ding, Y., Akopian, A.N., Stanfa, L., Suzuki, R., Carpenter, K., Dickenson, A., Boyce, S., Hill, R., Nebenuis-Oosthuizen, D., Smith, A.J., Kidd, E.J., Wood, J.N., 2000. Warm-coding deficits and aberrant inflammatory pain in mice lacking P2X3 receptors. Nature 407 (6807), 1015–1017. https://doi.org/10.1038/35039526
- Starowicz, K., Makuch, W., Korostynski, M., Malek, N., Slezak, M., Zychowska, M., et al., 2013. Full inhibition of spinal FAAH leads to TRPV1-mediated analgesic effects in neuropathic rats and possible lipoxygenase-mediated remodeling of anandamide metabolism. PLoS One 8 (4), e60040. https://doi.org/10.1371/journal.pone. 0060040.
- Todd, A.J., 2010. Neuronal circuitry for pain processing in the dorsal horn. Nat. Rev. Neurosci. 11 (12), 823–836. https://doi.org/10.1038/nrn2947.
- Tsou, K., Lowitz, K.A., Hohmann, A.G., Martin, W.J., Hathaway, C.B., Beriter, D.A., et al., 1996. Suppression of noxious stimulus-evoked expression of Fos protein-like immunoreactivity in rat spinal cord by a selective cannabinoid agonist. Neuroscience 70, 791–798. https://doi.org/10.1016/s0306-4522(96)83015-6.
- Tsujino, H., Kondo, E., Fukuoka, T., Dai, Y., Tokunaga, A., Miki, K., Yonenobu, K., Ochi, T., Noguchi, K., 2000. Activating transcription factor 3 (ATF3) induction by axotomy in sensory and motoneurons: a novel neuronal marker of nerve injury. Mol. Cell Neurosci. 15, 170–182. https://doi.org/10.1006/mcne.1999.0814.
- Viatchenko-Karpinski, V., Novosolova, N., Ishchenko, Y., Azhar, M.A., Wright, M., Tsintsadze, V., Kamal, A., Burnashev, N., Miller, A.D., Voitenko, N., Giniatulin, R., Lozovaya, N., 2016. Stable, synthetic analogs of diadenosine tetraphosphate inhibit rat and human P2X3 receptors and inflammatory pain. Mol. Pain 12. https://doi.org/ 10.1177/1744806916637704.
- Zeisel, A., Hochgerner, H., Lonnerberg, P., Johnsson, A., Memic, F., van der Zwan, J., Haring, M., Braun, E., Borm, L.E., La Manno, G., Codeluppi, S., Furlan, A., Lee, K., Skene, N., Harris, K.D., Hjerling-Leffler, J., Arenas, E., Ernfors, P., Marklund, U., Linarsson, S., 2018. Molecular architecture of the mouse nervous system. Cell 174 (4), 999–1014. https://doi.org/10.1016/j.cell.2018.06.021.